Nucleic Acids Research Advance Access published June 17, 2011

Nucleic Acids Research, 2011, 1–14
doi:10.1093/nar/gkr417

S1 ribosomal protein and the interplay between translation and mRNA decay

Francesco Delvillani, Giulia Papiani, Gianni Dehò and Federica Briani*

Dipartimento di Scienze biomolecolari e Biotecnologie, Università degli Studi di Milano, Via Celoria 26, 20133 Milano, Italy

Received March 16, 2011; Revised May 2, 2011; Accepted May 6, 2011

ABSTRACT

S1 is an 'atypical' ribosomal protein weakly associated with the 30S subunit that has been implicated in translation, transcription and control of RNA stability. S1 is thought to participate in translation initiation complex formation by assisting 30S positioning in the translation initiation region, but little is known about its role in other RNA transactions. In this work, we have analysed *in vivo* the effects of different intracellular S1 concentrations, from depletion to overexpression, on translation, decay and intracellular distribution of leadered and leaderless messenger RNAs (mRNAs). We show that the *cspE* mRNA, like the *rpsO* transcript, may be cleaved by RNase E at multiple sites, whereas the leaderless *cspE* transcript may also be degraded via an alternative pathway by an unknown endonuclease. Upon S1 overexpression, RNase E-dependent decay of both *cspE* and *rpsO* mRNAs is suppressed and these transcripts are stabilized, whereas cleavage of leaderless *cspE* mRNA by the unidentified endonuclease is not affected. Overall, our data suggest that ribosome-unbound S1 may inhibit translation and that part of the *Escherichia coli* ribosomes may actually lack S1.

INTRODUCTION

Decades of research in the model organism *Escherichia coli* have provided a deep knowledge of cellular machineries involved in translation and messenger RNA (mRNA) degradation; however, how these two processes are interconnected at the molecular level is still poorly understood. It is commonly accepted that translation deeply affects mRNA decay, as mutations that prevent or reduce translation usually shorten mRNA half-life. However, a relatively low number of studies have directly addressed the interplay between translation and RNA degradation and a small repertoire of model mRNAs have been analysed in this respect so far (1,2).

Serendipitous observations by different laboratories suggest that the ribosomal protein S1 could be involved in the crosstalk between protein synthesis and RNA degradation. S1 is the largest ribosomal protein in the 30S subunit of *E. coli* ribosome and is the only ribosomal protein with documented high affinity for mRNA (3). The protein has also been identified as a poly(A) tail binding factor from *E. coli* cell extracts (4) and shown to interact with RNase E and PNPase, two of the main *E. coli* RNA degrading enzymes, in Far-Western assays (5). Moreover, altering S1 expression from overexpression to depletion has opposite effects on mRNA expression, since S1 excess seems to stabilize different *E. coli* mRNAs that become barely detectable upon S1 depletion (6).

S1 has been considered a translation factor rather than a 'real' ribosomal protein, given its weak and reversible association with ribosomes (7,8) and its stoichiometry of less than one copy per 30S subunit (9). However, dissociation of S1 from the 30S subunit after cell lysis has been considered by different groups an experimental artefact, thus questioning the stoichiometry of the protein in the ribosome and the real magnitude of the non-ribosomal S1 pool (10–12). As a matter of fact, S1 is one of the few ribosomal proteins whose role in translation has been specifically analysed. *In vivo,* S1 is essential for growth and is required for translation of bulk mRNA in *E. coli* (6,13); on the other hand, ribosomes depleted of S1 and S2 retain the ability of translating the naturally leaderless λ *cI* and Tn*1721 tetR* mRNAs (14). Recently, it has been shown that a 'minimal' ribosome, lacking several proteins of the 30S subunit, among which S1, is still proficient in leaderless mRNA translation (15). *In vitro*, S1 is required for the assembly of 30S initiation complex at internal ribosome entry sites [i.e. located in 5′-untranslated region (UTR)] of mRNAs (16). It has been proposed that the interaction

*To whom correspondence should be addressed. Tel: +39 02 5031 5033; Fax: +39 02 5031 5044; Email: federica.briani@unimi.it
Present address:
Giulia Papiani, CNR, Istituto di Neuroscienze, Via Vanvitelli 32, 20129 Milano, Italy

between S1 in the 30S and the mRNA 5′-UTR may be responsible for a first, rapid and reversible step in initiation complex formation, which will be followed by the establishment of specific interactions between the Shine–Dalgarno (SD) and 16S rRNA (17,18). However, S1 is dispensable for initiation complex formation on RNAs with a strong SD region (19) or on leaderless mRNAs. In fact, initiation of leaderless mRNA translation occurs *in vitro* through a non-conventional pathway by direct binding to the 70S ribosome (14,20,21). This 70S-dependent initiation pathway seems to be, at least *in vitro*, insensitive to the presence of S1, since it occurs with ribosomes devoid of both S1 and S2 (as a consequence of an *rpsBts* mutation) and with crosslinked 70S ribosomes still containing S1 and S2 (20). It has been reported that also *in vivo*, in conditions where 70S ribosomes become prevalent because of a mutation that impairs ribosome recycling factor activity, leaderless mRNAs are translated whereas translation of bulk mRNA ceases (20). It is not known whether the 70S particles that accumulate in the mutant still retain S1.

S1 binding sites on mRNA have been recognized as A/U- rich single-stranded regions usually located immediately upstream of the SD (22,23). Interestingly, those regions constitute RNase E cleavage sites in different mRNAs (1). Nevertheless, the insertion of AU-rich elements upstream of an SD sequence enhances translation and stabilizes mRNA, suggesting that ribosome assembly on the mRNA via S1 binding may prevent RNase E cutting (24). It remains to be established, however, whether *in vivo* S1 not bound to the ribosome may also interact with mRNA and regulate its decay.

We have previously shown that both S1 overexpression and depletion inhibit bacterial growth but have different outcomes on mRNA expression (6). We observed that upon S1 depletion, the amount of several mRNAs sharply decreased; conversely, the quantity of most mRNAs did not significantly change or increase in S1 over-expressing cells. However, upon S1 overexpression, all the assayed mRNAs became notably more stable than in S1 basal expression condition. Surprisingly, the exonuclease polynucleotide phosphorylase (PNPase) seemed to enhance S1 protective effect for most of the assayed mRNAs.

In this work, we have investigated the role of mRNA association with the ribosome and translation on S1-dependent modulation of mRNA stability. Our data suggest that S1 may specifically inhibit RNase E-dependent decay by hindering RNase E cleavage sites.

MATERIALS AND METHODS

Bacterial strains and plasmids

Bacterial strains and plasmids are listed in Supplementary Table S1. *Escherichia coli* sequence coordinates are from NCBI Accession Number U00096.2. C-1a (25), C-5868 and C-5869 (26) have been previously described. C-5699 is a C-5698 derivative (6) in which the *cat* resistance cassette was excised by FLP-mediated recombination as described (27). C-5874 was obtained by P1 transduction of the Δ*cspE*::*kan* allele from JW0618 [Keio collection; (28)] into C-1a; the resistance cassette was then excised by FLP-mediated recombination. C-5899 and C-5901 were obtained by P1 transduction of the Δ*rng*::*kan* and Δ*elaC*::*kan* alleles from JW3216 and JW2263 strains [Keio collection; (28)], respectively, in C-5868.

pQE31-S1 and pREP4 were kindly provided by M. V. Sukhodolets. The recombinant S1 protein expressed from pQE31-S1 allele carries an N-terminal His6 tag (29). The other plasmids used in this work (see also Figure 2A) are derivatives of pGM385. This plasmid was obtained by cloning in the XbaI site of pGM743 vector (30,31) a 170-bp-long DNA fragment carrying the bacteriophage P4 Rho-dependent transcription terminator t_{imm} (GenBank Accession Number X51522: 8365-8209) (32). Coordinates of the *E. coli cspE* fragments cloned in pGM385 are reported in Supplementary Table S1. In plasmids pGM928 and pGM929, the HA epitope coding fragment (TACCCATACGACGTCCCAGACTACGCT) has been inserted in frame within the *cspE* coding region. Plasmids pGM396 and pGM398 carry the *rpsO* gene with or without the 5′-UTR, respectively. The *rpsO* region essential for the interaction with the ribosome (33) has been deleted in these plasmids and replaced with the in frame HA epitope DNA, flanked by NheI and SacI restriction sites. Plasmid pGM397 is a pGM396 derivative in which the *rpsO* region upstream of the HA has been replaced by an in frame phage λ DNA fragment carrying P_{RM} and the first 189 bp of *cI* open reading frame (ORF). It should be mentioned that plasmid pGM396 rearrangements have been found in a significant percentage of transformed cells, probably because of the toxicity of the hybrid RpsO-HA protein. On the contrary, plasmid rearrangements were never observed after transformation with plasmids pGM397 and pGM398. All fragments were obtained by polymerase chain reaction (PCR) on MG1655 (34) or λ genomic DNA with suitable oligonucleotides, sub-cloned by standard molecular biology techniques and checked by sequencing.

LD broth (35) was supplemented with chloramphenicol (30 μg/ml), ampicillin (100 μg/ml) and kanamycin (50 μg/ml) when needed.

Modulation of S1 expression in *E. coli* cultures

For S1 overexpression, strains harbouring both pQE31-S1 and pREP4 plasmids were grown at 37°C in LD broth in a reciprocating waterbath until $OD_{600} = 0.4$ was reached. The cultures were then split in two, 1 mM isopropyl-β-D-thiogalactopyranoside (IPTG) was added to one of the subcultures and incubation was continued at 37°C. Samples were taken at different times for RNA extraction or crude extracts preparation. S1 depletion was achieved in the *araBp-rpsA* conditional expression mutant C-5699. The strain was grown in LD broth supplemented with 1% arabinose (permissive condition) at 37°C in a reciprocating waterbath up to $OD_{600} = 0.2$. The cells were then collected by centrifugation, washed with 1vol of LD and diluted 4-fold in LD with 0.4% glucose (non permissive-depletion condition). Incubation at 37°C was then

continued until the culture stopped growing (around OD_{600} = 0.4–0.5).

Northern blotting and primer extension

Procedures for RNA extraction, northern blot analysis, synthesis of radiolabelled riboprobes by *in vitro* transcription with T7 RNA polymerase and 5′-end labelling of oligonucleotides with T4 polynucleotide kinase in the presence of [γ-^{32}P]ATP were previously described (36,37). As a loading control, urea-polyacrylamide gels were routinely stained with ethidium bromide before blotting and the intensity of the 5S rRNA band was evaluated with Quantity One (Bio-Rad) software. Coordinates of the CSPE riboprobe specific for *cspE* mRNA were 656576-656704. The oligonucleotide probes used in northern blotting experiments were: HA, 2135 (*cspE* ORF 3′-end), 2399 (*cspE* ORF 5′-end), 2313 (*rpsO* ORF), 2469 (*rpsO* leader) and 2521 (*rpsO* chromosomal allele). Autoradiographic images and densitometric analysis of northern blots were obtained by phosphorimaging using ImageQuant software (Molecular Dynamics). mRNA half-lives were estimated as described (6) by regression analysis of mRNA remaining (calculated as the densitometric signal at a given time) versus time after rifampicin addition.

Primer extension was performed on 10 µg of RNA extracted from different strains, as detailed in Figure 3B and Supplementary Figure S4 legends, with either the 5′-end ^{32}P-labelled 2174 (internal to *cspE* ORF) or HA oligonucleotides as previously described (38).

Analysis of protein and mRNA distribution in cell fractions

Escherichia coli cultures expressing S1 at different levels were grown as detailed above, whereas strains with autogenously regulated S1 were grown at 37°C in LD broth in a reciprocating waterbath until OD_{600} = 0.7–0.8 was reached. Preparation of crude extracts was performed as described by Charollais *et al*. (39) by freeze thawing in buffer A (10 mM Tris–HCl, pH 7.5, 60 mM KCl, 10 mM $MgCl_2$). The extract concentration was estimated by measuring the OD_{260}. Ribosomes and ribosomal subunits were prepared by centrifugation of the lysate at 100 000*g* for 2 h at 4°C. The supernatant (S100 fraction) was taken and the pellet was carefully washed and resuspended in one volume of buffer A. RNA was prepared by phenol–chloroform extraction from equal volumes of crude extract before ultracentrifugation (total), pellet (ribosomal fraction) and supernatant (S100). After ethanol precipitation of RNA, the samples were resuspended in identical volumes of RNase-free water.

To analyse the polysome profile, 14 OD_{260} units of the crude extracts were layered onto a 10–40% (w/v) sucrose gradient in 10 mM Tris–HCl, pH 7.5, 50 mM NH_4Cl, 10 mM $MgCl_2$, 1 mM dithiothreitol (DTT) and centrifuged at 35 000 r.p.m. for 2.5 h at 4°C in a Beckman SW41 rotor. After centrifugation, 0.2 ml fractions were collected and their OD_{260} was plotted. The areas of the peaks corresponding to S100 (top of the gradients), ribosomal subunits, monosome and polysome fractions were estimated by weighting. Ten microlitres of selected fractions were then assayed by western blotting with antibodies specific for L4 ribosomal protein (kindly provided by C. Gualerzi) to confirm the correspondence of the peaks with ribosomal subunits, monosomes and polysomes, and with S1 specific antibodies (kindly provided by U. Bläsi). The immunoreactive bands were revealed by Immobilon (Millipore) reagents and quantified with the ImageQuant software. S1 densitometric values were normalized to the highest value obtained and plotted on the ribosomal profile chart. For *cspE* mRNA analysis, 20 OD_{260} of crude extracts were loaded on sucrose gradients and fractionated as described above. Each strain and condition tested was prepared in duplicate and ultracentrifuged together. Corresponding 0.3 ml fractions of duplicate gradients were pooled and the OD_{260} of the fractions measured. S1 was quantified in a subset of such samples by western blotting as described above. RNA was prepared by phenol–chloroform extraction of 0.3 ml of selected pooled fractions; after ethanol precipitation, the samples were resuspended in 0.15 vol of RNase-free water. Identical volumes of each RNA sample were analysed by northern blotting.

Electrophoretic mobility shift assay and *in vitro* degradation assays

The RNA probes used in electrophoretic mobility shift assay (EMSA) and *in vitro* degradation assays were synthesized by *in vitro* transcription of proper DNA fragments with T7 RNA polymerase following the protocol recommended by the enzyme manufacturer. The DNA templates were obtained by PCR on MG1655 genomic DNA with oligonucleotides 2299 (complementary to the 3′-part of *cspEt*) and oligonucleotides 2434 (T7 promoter + *cspE* 656473-656495) for *cspE*$^+$ or 2433 (T7 promoter + *cspE* 656453-656472) for Δ*L-cspE*. In order to obtain uniformly labelled probes, the reactions were carried out in the presence of [α-^{32}P] CTP. 5′-labelled RNA probes were prepared by dephosphorylation with alkaline phosphatase of unlabelled probes, followed by phosphorylation with T4 polynucleotide kinase and [γ-^{32}P] ATP. For gel retardation assays, 0.7 fmol of each probe was incubated for 20 min at 21°C in binding buffer [50 mM Tris–HCl pH 7.4, 50 mM NaCl, 0.5 mM DTT, 0.025% NP40 (Fluka), 10% glycerol] with increasing amounts of purified S1 protein in a final volume of 10 µl. The samples were run on 5% native polyacrylamide gel at 4°C. After run, the gel was dried and analysed by phosphorimaging. The signals were quantified using ImageQuant (Molecular Dynamics) software. For *in vitro* degradation experiments, 1.2 pmol of *in vitro* transcribed radiolabelled *cspE*$^+$ or Δ*L-cspE* RNA were incubated in 10 mM Tris–HCl pH 7.4, DTT 0.75 mM, Mg Acetate 4.5 mM, KCl 10 mM with 30 ng of RNA degradosome (prepared as described in ref. 40) at 26°C in a final volume of 15 µl. The experiment was performed in the absence of phosphate and NDPs, so as to prevent PNPase exonucleolytic and polymerization activities. Samples (3 µl) were removed at different time points and the reaction was stopped by adding 5 µl of RNA loading dye [2 mg/ml XC and BBF, 10 mM

ethylenediaminetetraacetic acid (EDTA) in formamide]. The samples were run on a 6% acrylamide denaturing gel. The gel was dried and analysed by phosphorimaging.

RESULTS

S1 ribosomal protein intracellular distribution is affected by S1 overexpression and depletion

Both S1 depletion and overexpression impair bacterial growth, presumably because altered S1 levels may affect translation (6,13). However, whereas translation inhibition is an expected outcome of S1 depletion, as S1 seems to be involved in translation initiation of most mRNAs (13), the effect of S1 overexpression on translation is far less obvious. To better understand the consequences of different S1 intracellular levels, we analysed the polysome profile and the intracellular distribution of S1 after modulating its expression from depletion to overexpression. Crude cell extracts were fractionated by ultracentrifugation on sucrose gradient and the polysome profile was assessed as described in 'Materials and Methods' section (Supplementary Table S2). Selected fractions were analysed by western blotting with anti-S1 antibodies and the signals quantified by densitometry. The results are shown in Figure 1A. In conditions of physiologically regulated S1 expression (S1 basal), S1 is present in the top (S100 S1), 30S, monosome and polysome fractions. S1 overexpression led to a drastic decrease of polysomes and ribosomal subunits and to accumulation of monosomes. A similar profile was observed in S1-depleted cells (S1 depletion), albeit in this case the polysome and ribosomal subunit peaks reduction was less severe. It should be reminded that in the latter condition S1 did not completely disappear even at late time points after shift to non-permissive conditions (6). Western blotting analysis of the fractions showed that the amount of S1 not associated to ribosomes (top fractions) clearly increased upon overexpression of the protein. On the contrary, upon S1 depletion, S1 was found only in 30S, monosome and residual polysomes fractions, whereas it was absent in the top fractions of the gradient (Figure 1A). We measured the amount of S1 relative to ribosomal protein L4 and to PNPase, taken as loading controls for 70S and free fractions, respectively, by western blotting of selected fractions (indicated by the arrows in Figure 1A). As can be seen in Figure 1B, variation of S1 expression strongly affected the non-ribosomal S1 pool; however, upon overexpression S1 slightly increased also in the monosomes whereas it sharply decreased in depleted cells (Figure 1B). It should be mentioned that the presence in the monosome fraction of PNPase, which was used in this experiment as a loading control, is presumably due to its association to the high molecular weight complex RNA degradosome, since in the *rne-131* mutant, which encodes a C-terminally truncated RNase E that does not assemble the degradosome (41,42), PNPase was found only in the top fractions (Supplementary Figure S1).

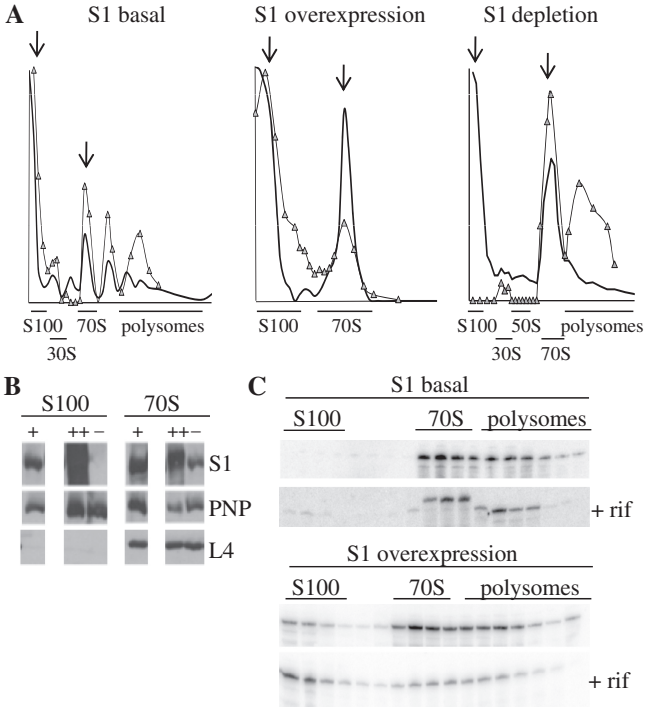

Figure 1. Ribosomal profile and intracellular distribution of S1 and *cspE* mRNA. Crude cell extracts were prepared as detailed in 'Materials and Methods' section from the following strains and conditions. S1 basal: C-1a exponential culture grown up to OD_{600} = 0.8; S1 overexpression: C-1a/pQE31S1/pREP4 was grown up to OD_{600} = 0.4 and incubated 60 min with 1 mM IPTG to induce *rpsA* transcription; S1 depletion: C-5699 (*araBp-rpsA*) grown up to OD_{600} = 0.2 in permissive conditions (LD +arabinose) was diluted 1 : 4 in non-permissive conditions (LD +glucose) to switch off *rpsA* transcription and further incubated for about 120 min. Cultures were grown at 37°C; before collecting the cells, the cultures were incubated 5 min at 37°C with chloramphenicol (final concentration, 0.1 mg/ml) to prevent polysome dissociation (39). Crude cell extracts (14 OD_{260}) were then fractionated by ultracentrifugation on 10–40% sucrose gradients. (**A**) Ribosomal profile. Thick continuous line: OD_{260} measured for each gradient fractions; grey triangles: S1 distribution. Ten microlitres of the indicated fractions were assayed by western blotting with S1-specific antibodies and the densitometric values (obtained as described in 'Materials and Methods' section) were normalized for the highest value obtained. (**B**) Distribution of S1, PNPase and ribosomal protein L4 in the S100 and 70S fractions. 0.02 OD_{260} of S100 and 70S fractions indicated by arrows in (A) were analysed by western blotting with specific antibodies (as indicated beside the panels). +, S1 basal; ++, S1 overexpression; −, S1 depletion. (**C**) Intracellular distribution of *cspE* mRNA. For extracts preparation, 100 ml of culture were taken before and 25 min after addition of 0.4 mg/ml rifampicin and 0.03 mg/ml nalidixic acid (+ rif). RNA was extracted from equal volumes of selected fractions; identical aliquots of RNA samples were loaded on a 6% denaturing polyacrylamide gel and analysed by northern blotting with the CSPE riboprobe. The altered electrophoretic mobility of *cspE* transcripts observed in the 70S samples (S1 basal, + rif) is probably imputable to the high concentration of ribosomal RNA in those fractions, since these transcripts migrated with the expected mobility upon sample dilution (data not shown).

S1 overexpression decreases the fraction of ribosome-associated *cspE* mRNA

To clarify whether mRNA stabilization upon S1 overexpression differentially affected ribosome-bound or unbound transcripts, we analysed the intracellular

distribution and stability of *cspE* mRNA relative to the ribosomes. We chose the *cspE* mRNA as a model because it is highly expressed and subject to S1-dependent stabilization (6). Crude extracts of S1 overexpressing and control (physiologically regulated *rpsA*) cultures immediately before and 25 min after rifampicin addition were fractionated on sucrose gradients. In the control gradients (Figure 1C, S1 basal), the *cspE* mRNA was found in monosome and polysome fractions; a tiny amount of mRNA (~0.2%; calculated by densitometry of the northern signals) was also detected upon longer exposure in the top fractions together with shorter RNAs, presumably *cspE* transcript degradation fragments (data not shown). After incubation with rifampicin, the polysomes disassembled and the 70S peak size increased (data not shown), in agreement with previously published data (43). Although most of the residual mRNA (on the whole, about one-tenth of the initial amount of RNA) was still located in the monosome and residual polysome fraction, the relative amount of the *cspE* transcript in the top versus ribosomal fractions increased almost 6-fold, as assessed by densitometric analysis of the signals (Figure 1C, S1 basal, +rif). In S1 over-expressing cells (Figure 1C, S1 overexpression), most mRNA appeared to be associated with monosomes and polysomes; however, the mRNA was readily detected in the top fractions before addition of rifampicin. Also in this case, after the incubation with the antibiotic, the relative amount of the *cspE* transcript at the top of the gradient significantly increased (from about 7% to 40%). It thus appears that the increased stability of *cspE* mRNA may be mainly attributed to the higher fraction of ribosome unbound transcripts.

S1 expression modulation differently affects leaderless and leadered transcript stability

It has been proposed that single-stranded regions in 5′-UTRs may constitute preferential S1 binding sites (22,23). To test whether the 5′-UTR was relevant for S1-dependent modulation of mRNA stability, we analysed in different conditions of S1 expression the transcript pattern of a *cspE* allele devoid of its leader region (Δ*L-cspE*) ectopically expressed from its natural *cspEp* promoter (plasmid pGM924, Figure 2A); as assessed by primer extension (Figure 3B), the Δ*L-cspE* primary transcript started with the gene start codon. In the northern blotting experiments shown in Figure 3A, we observed that when S1 expression was physiologically regulated, the leaderless transcript (Δ*L-cspE*) was much less stable than the leadered RNA ($cspE^+$) (half-life of <1 min for the Δ*L-cspE* versus about 4 min for the chromosomal $cspE^+$). Upon S1 overexpression, both transcripts were stabilized; in addition, several shorter RNAs were detected by the probe (Table 1 and Figure 3A). These short transcripts derived from degradation of the leaderless mRNA since they were not detectable in the wild-type strain lacking the plasmid (6), whereas they were produced in the Δ*cspE* chromosomal mutant carrying pGM924 (Figure 3A, right panel). Such short transcripts terminate downstream of the *cspE* stop codon, probably at the gene intrinsic terminator, and differ at their 5′-ends, as assessed by northern

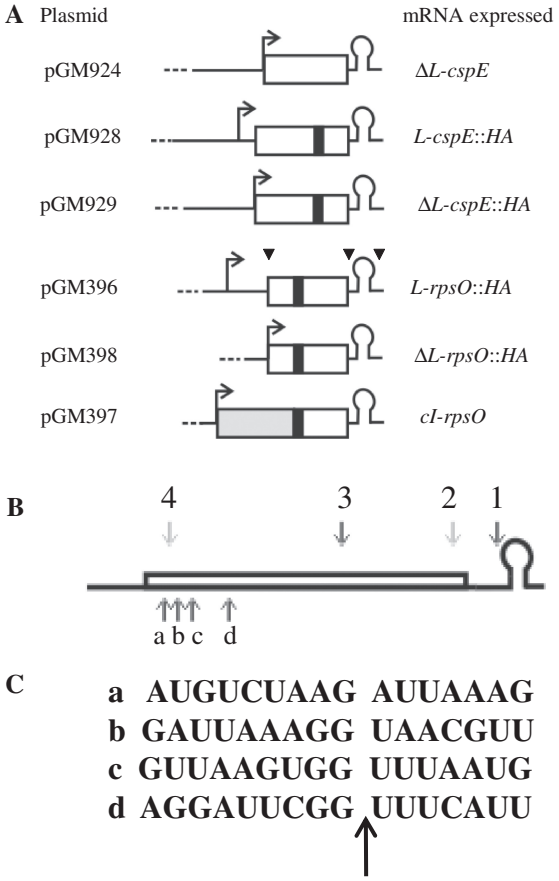

Figure 2. Map of plasmid-encoded *cspE* and *rpsO* alleles and of endonucleolytic cleavage sites on *cspE* mRNA. (**A**) Map of *cspE* and *rpsO* alleles cloned in pGM385 plasmid vector. Details about plasmid construction and coordinates of the cloned regions are reported in 'Materials and Methods' section. Transcription from *cspEp* and *rpsOp* promoters starts at nucleotide 657 473 and 3 309 808, respectively; coordinates of the palindromic region of *cspEt* and *rpsOt* transcription terminators are 656 744–656 768 and 3 309 420–3 309 394 (45,69). The promoters, 5′-UTRs and coding regions of the model genes are drawn to scale, whereas 3′-UTRs elements are reported on an arbitrary scale. Dotted line, vector sequence; bent arrow, promoters; hairpin, Rho-independent terminator; black box, HA epitope coding region. The *cspE* constructs carry the *cspEp* constitutive promoter. The grey box in pGM397 represents phage λ *cI* 5′ region. In pGM396 and pGM398, transcription of *rpsO*::HA alleles is driven by the *rpsOp* promoter; in pGM398, the 5′-UTR of *rpsO* was deleted and the transcript from *rpsOp* produced by the plasmid started with the A of the AUG of the gene (as assessed by primer extension; Supplementary Figure S4). In pGM397, the *rpsOp* and the 5′-end of the ORF, up to the HA insertion point, were replaced by P_{RM} and the first 63 codons of λ *cI* gene, which is naturally leaderless when transcribed from that promoter (70). The black triangles above pGM396 indicate the position of three RNase E cleavage sites mapped in *rpsO*, M2 (immediately upstream of the *rpsOt* terminator), M3 (at the beginning of *rpsO* coding sequence) and M sites (overlapping *rpsOt*) (69,71,72). (**B**) Map of endonucleolytic cleavage sites on *cspE* mRNA. Upward arrows: *in vivo* cleavage sites on Δ*L-cspE*; the 5′ ends of degradation products were mapped by primer extension (Figure 3B). Downward arrows: *in vitro* RNase E-cleavage sites detected on both leadered $cspE^+$ and Δ*L-cspE* (black arrows) or on either $cspE^+$ (site 4; data not shown) or Δ*L-cspE* (site 2) (grey arrows; see Figure 4B). (**C**) Nucleotide sequence associated with cut sites observed *in vivo*. The position of the listed sites in *cspE* mRNA is shown in (B) above. The arrow indicates the cleavage position.

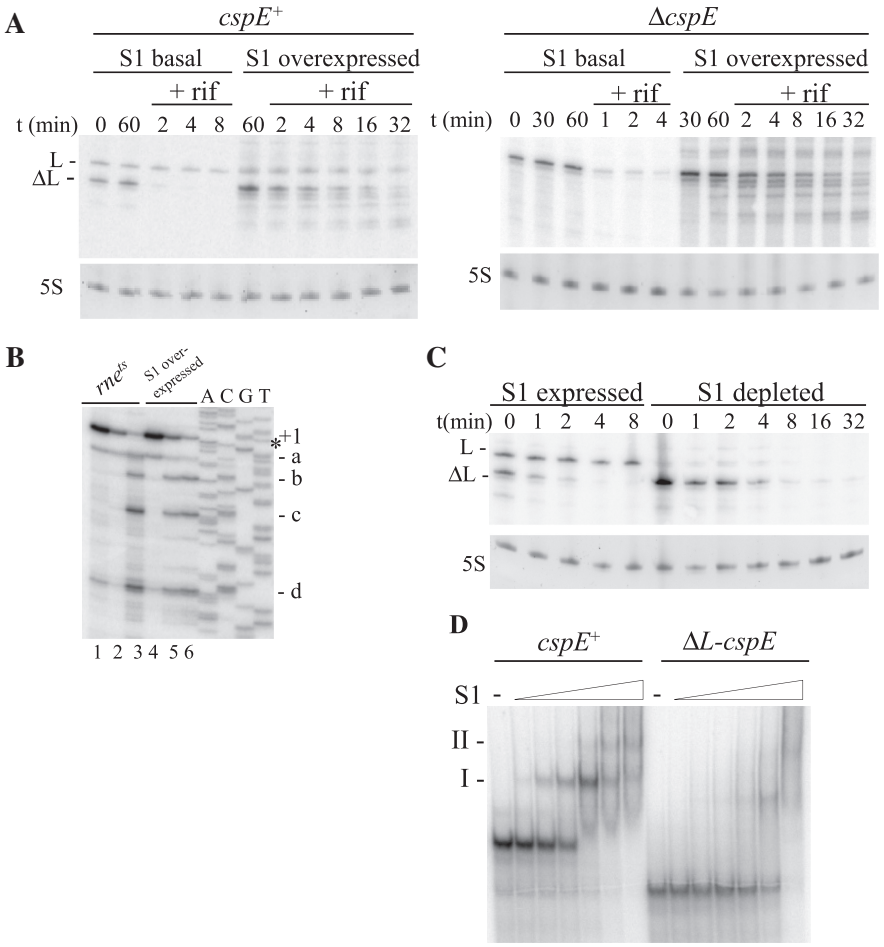

Figure 3. Analysis of leadered and leaderless *cspE* alleles transcripts. (**A**) Expression and stability of leadered and leaderless *cspE* mRNA upon S1 overexpression. Exponential cultures of C-1a/pREP4/pQE31-S1/pGM924 (*cspE*$^+$) or C-5874/pREP4/pQE31-S1/pGM924 (Δ*cspE*) ectopically expressing the leaderless *cspE* allele from pGM924 were grown up to OD_{600} = 0.4 (time = 0) and split in two subcultures. In one subculture (S1 over-expressed) S1 expression was induced by 1 mM IPTG addition and after 60 min (time = 60) the cultures were treated with rifampicin (0.4 mg/ml) and nalidixic acid (0.03 mg/ml). Aliquots for RNA extraction were sampled at times 0 and 60 (no antibiotics) and at different time points after addition of the antibiotics, as indicated (in min) on top of the lanes. Northern blotting was performed as described in 'Materials and Methods' section after 6 % denaturing polyacrylamide gel electrophoresis of 5 µg of RNA samples hybridized with radiolabelled CSPE riboprobe (upper panels). (Bottom panels) the gel was stained with ethidium bromide before transfer to check the amount of the loaded RNA samples. The gel portion with 5S rRNA signals is shown. L, leadered *cspE* chromosomal transcript; ΔL, leaderless *cspE* plasmid transcript. (**B**) Primer extension on leaderless *cspE* RNA degradation products. Selected RNA samples extracted from cultures of C-5868/pGM924 (grown as described in Figure 4A legend) and C-5874/pREP4/pQE31-S1/pGM924 (grown as described here above) were analysed by primer extension with oligonucleotide 2174, as described in 'Materials and Methods' section. The positions of different 5′-ends (a, +10; b, +18; c, +31 and d, +54) relatively to the first A of the primary transcript (+1) were defined by running the samples along with DNA sequencing reactions obtained with the same oligonucleotide and plasmid pGM924. The star beside the sequence indicates the A in the AUG initiation codon of *cspE* gene.1, C-5868/pGM924, 32°C, time 0; 2 and 3, 44°C, 0 and 4 min after rifampicin addition; 4, 5 and 6, C-5874/pREP4/pQE31-S1/pGM924 before (4) and 60 min after (5 and 6) S1 induction by IPTG. Samples 4 and 5 were taken before rifampicin addition (time 0), sample 6, 4 min after. (**C**) S1 depletion. Bacterial cultures of C-5699/pGM924 were grown up to OD_{600} = 0.4, diluted 1:4 in permissive (+ arabinose, S1 expressed) or non-permissive (+ glucose, S1 repressed) conditions and further incubated until OD_{600} = 0.4–0.5 was reached. RNA was extracted from rifampicin-nalidixic acid treated and untreated samples and northern blotted with radiolabelled 2135 oligonucleotide, as described above (upper panel). (Bottom panel) Ethidium bromide-stained 5S rRNA. L, leadered *cspE* chromosomal transcript; ΔL, leaderless *cspE* plasmid transcript. (**D**) EMSA with purified S1. Radiolabelled *cspE*$^+$ and Δ*L-cspE* RNAs were synthesized *in vitro* in the presence of [α^{32}P]-CTP. The probes (0.7 nM) were incubated 20 min at 21°C without (−) and with increasing amount of S1 (0.1, 0.5, 2.5, 5 and 25 nM). The samples were run on a 5% native polyacrylamide gel.

blotting with oligonucleotides specific for the 3′- and 5′-end (Supplementary Figure S2) and by primer extension analysis (Figure 3B). The position of the different 5′-ends detected and the nucleotide sequence of the cut sites are reported in Figure 2B and C, respectively.

Upon S1 depletion, the *cspE*$^+$ transcript became almost undetectable (6), whereas Δ*L-cspE* became more abundant and stable (Table 1 and Figure 3C). It should be noted that only the primary transcript but not the decay intermediates was stabilized in this condition.

We also assessed S1 ability to bind *in vitro* either the leadered or the leaderless *cspE* RNAs by EMSA. As shown in Figure 3D, His-tagged S1 formed two complexes with the *cspE*$^+$ transcript: complex I, which formed at S1 concentration as low as 0.1–0.5 nM, and complex II, which migrated more slowly than complex I and could

Table 1. mRNA expression and stability upon S1 depletion and overexpression

mRNA	S1 depletion[a]			S1 over-expression[a]		
	R.A.[b]	mRNA half-life (min)[c]		R.A.[b]	mRNA half-life (min)[c]	
		ARA	GLU		−IPTG	+IPTG
cspE^{+}[d]	0.2 ± 0.0	>4.0	2.5 ± 0.7	1.2 ± 0.1	7.2 ± 1.1	24.4 ± 4.7
Δ*L-cspE*[e]	2.9 ± 0.3	0.8 ± 0.3	2.0 ± 0.8	1.4 ± 0.5	0.6 ± 0.3	5.7 ± 0.5
rpsO^{+}[d]	0.2 ± 0.1	1.8 ± 0.2	1.6 ± 0.0	0.2 ± 0.1	1.8 ± 0.4	11.3 ± 2.1
Δ*L-rpsO::HA*[f]	3.1 ± 0.6	0.6 ± 0.0	1.0 ± 0.3	2.6 ± 0.2	1.2 ± 0.3	14.6 ± 5.8
cI-rpsO[g]	2.0 ± 0.4	1.0 ± 0.1	1.8 ± 0.1	3.2	1.0	9.4

[a]Cultures of C-5699 (S1 depletion) or C-1a/pQE31-S1/pREP4 (S1 overexpression) were grown and experiment performed as detailed in Figure 3 and Supplementary S5 legends and in 'Materials and Methods' section.
[b]Relative abundance, calculated as the ratio between mRNA amounts in cultures incubated with glucose and arabinose immediately before rifampicin addition (S1 depletion) or between induced and non-induced cultures 60 min after IPTG addiction (S1 overexpression).
[c]Calculated as detailed in 'Materials and Methods' section; the reported values represent average and standard deviation of at least two independent determinations in all cases, but the *cI-rpsO* mRNA in S1 overexpression, for which they are the results of a single determination.
[d]Leadered mRNAs. Cultures carrying either pGM924 (*cspE*) or pGM398 (*rpsO*) plasmid. mRNA expressed from chromosomally encoded alleles were considered for half-life calculation. For *rpsO*$^{+}$, only the mRNA terminated at *rpsOt* was considered. Albeit the stabilization factor for *rpsO*$^{+}$ mRNA by over-expressed S1 is in agreement with previous determinations performed in our laboratory, the half-life absolute values and especially the relative abundance (R.A.) reported here differ considerably from published data (6). This discrepancy is probably due to technical reasons, since data reported here refer to a single mRNA specie (the *rpsOp-rpsOt* mRNA) sharply resolved in polyacrylamide gel with very low background (see Supplementary Figure S5), whereas previously published data concerned the sum of two puffy agarose gel signals with high background (6).
[e,f,g]Leaderless alleles. Cells carrying pGM924 (e), pGM398 (f) or pGM397 (g) plasmid. Only signals corresponding to the primary transcripts (from *cspEp* to *cspEt*, e, *rpsOp-rpsOt*, f, and P_{RM}-*rpsOt*, g) expressed by the plasmids were considered for R.A. and half-life determination.

be detected at S1 concentrations ≥2.5 nM. Retardation of the leaderless transcript, on the contrary, occurred only at high (≥2.5 nM) S1 concentrations. This suggests that a high-affinity-binding site, responsible for complex I formation, may be present in the *cspE*$^{+}$ probe and missing in Δ*L-cspE*.

S1 inhibits RNase E-dependent decay *in vivo*

RNase E is thought to initiate the decay of several mRNAs by endonucleolytic cleavages at their 5′-end (44) and has been implicated in degradation of *cspE* mRNA (45,46). To test if Δ*L-cspE* mRNA decay products observed upon S1 overexpression could be generated by this enzyme, we analysed the transcription profile of the Δ*L-cspE* allele in an RNase E thermosensitive mutant. As shown in Figure 4A and summarized in Supplementary Table S3, in the *rne*^{ts} strain at 44°C the transcription profile of both the leadered (chromosomal) and the leaderless (plasmid-encoded) *cspE* alleles was strikingly similar to the pattern observed upon S1 overexpression, as both transcripts were stabilized and several shorter RNAs were detected after rifampicin addition, a condition that seems to exacerbate the RNase E-defective phenotype of *rne*^{ts} strains (47). These shorter decay products appeared to correspond to the Δ*L-cspE* decay intermediates that were stabilized in S1 over-expressing cells, since they: (i) were not detected in the absence of the plasmid pGM924; (ii) had identical 5′-ends, as assessed by primer extension, and exhibited the same electrophoretic mobility as those observed upon S1 overexpression; and (iii) hybridized with an oligonucleotide overlapping the *cspE* stop codon (Figure 3B and data not shown). Such degradation intermediates were still detected in the double *rne*^{ts} Δ*rng* mutant (lacking RNase G, a paralogue of RNase E with the same propensity to cleave within AU-rich single-stranded segments) (48), and in the double *rne*^{ts} Δ*elaC* mutant, lacking a functional RNase Z previously implicated in *cspE* mRNA decay (46) (Supplementary Figure S3), thus ruling out that these two nucleases are implicated in generation of such decay intermediates. The alignment of cleavage sites shows that the cut invariably occurs after a G residue embedded in a U-rich sequence. To our knowledge, none of the known *E. coli* endoribonucleases exhibits such cleavage specificity. Narrow substrate specificity is typical of mRNA interferases, which are components of toxin–antitoxin systems (49). S1 is known to stimulate the activity of bacteriophage T4 RegB endoribonuclease (50,51) which has structural similarities with two *E. coli* interferases, YoeB and RelE (52).

It thus appears that the leaderless Δ*L-cspE* transcript may be degraded by two pathways: an RNase E-dependent pathway that is inhibited by S1 overexpression and an alternative processing by an unidentified endonuclease, which is not prevented by S1. It will be interesting to identify such endonuclease and to analyse whether S1 may play a positive role in this degradation pathway.

To identify *in vitro* RNase E cleavage sites in both leadered *cspE* and Δ*L-cspE*, we digested these RNAs with purified RNA degradosome in conditions that prevented PNPase enzymatic activities. We performed this experiment with either 5′-radiolabelled (Figure 4B, left) or (Figure 4B, right) uniformly labelled probes. Monophosphorylated *cspE* and Δ*L-cspE* were degraded about 2-fold faster than ppp-mRNAs (assessed by plotting the amount of full-length substrate remaining at each time point; data not shown), suggesting that the degradation rate of our probes was only marginally affected by their phosphorylation state (53–55). Two main decay fragments

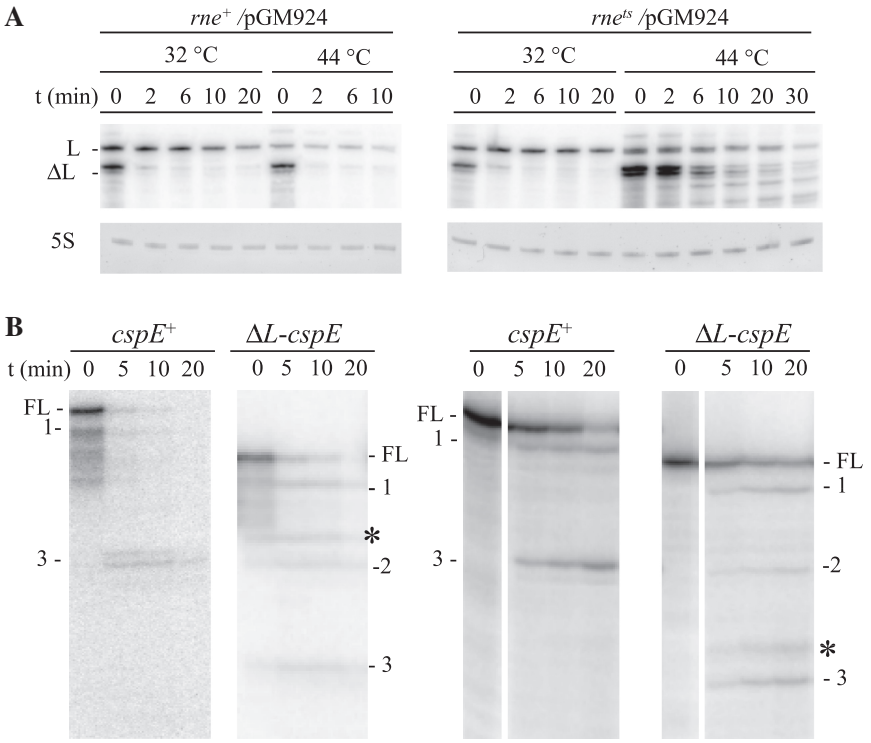

Figure 4. Analysis of RNase E role in $cspE^+$ and ΔL-*cspE* degradation. (**A**) *In vivo* analysis. Cultures of rne^+ (C-5869) and rne^{ts} (C-5868) strains carrying pGM924 were grown to mid-log phase at permissive temperature (32°C) and shifted at non-permissive temperature (44°C). Rifampicin was added immediately before (32°C samples) and 30 min after temperature shift (44°C) and RNA was extracted at the time points indicated on top of the lanes. Five micrograms of RNA samples were analysed by northern blotting with radiolabelled 2135 oligonucleotide. L, leadered *cspE* chromosomal transcript; ΔL, leaderless *cspE* plasmid transcript (upper panels). (Bottom panels) ethidium bromide-stained 5S rRNA. (**B**) *In vitro* degradation assay. $cspE^+$ and ΔL-*cspE* RNAs (35 nM) 5′-end ^{32}P-labelled (left) or uniformly radiolabelled with [α^{32}P]-CTP (right) were incubated at 26°C for the time indicated (in min) above the lanes with 60 ng of purified RNA degradosome and fractionated by 6% PAGE. The size of the main RNA species was estimated by running the samples along with a sequence ladder (data not shown). The corresponding leadered and leaderless RNAs are denoted by the same figure; their respective size (in nucleotides) and 3′-ends (coordinates from NCBI Accession Number U00096.2.) are as follows: 1: 270/229, 656742; 2: 169 (leaderless only), 656 683; 3: 165/127, 656 638. The stars indicate signals that were not reproducibly detected in other experiments. Shorter decay fragments migrating at the bottom of the gel (not shown in the figure), probably corresponding to the probes 3′-end fragments, were present in the right panel.

were visible. The 3′-end of these fragments were mapped (by comparison with a sequencing ladder; data not shown) immediately upstream of the intrinsic terminator *cspEt* and internally to the ORF, respectively (Figures 2B and 4B, signals 1 and 3). An additional 3′-end internal to the ORF was generated only with ΔL-*cspE* RNA (Figures 2B and 4B, signal 2). Other signals occasionally observed (Figure 4B, stars) may represent unstable degradation intermediates. Among them, an additional cut occurring 50/51-nt downstream of the 5′-end was detected with the *cspE* probe (Figure 2B, signal 4; data not shown). Signals corresponding to RNA molecules processed at upstream sites were never observed. Therefore, *in vitro* RNase E cleavage sites and *in vivo* cuts detected upon S1 overexpression or RNase E thermal inactivation map in different regions of the leaderless *cspE* mRNA (Figure 2B). Addition of purified His-tagged S1 to the *in vitro* degradation assay did not consistently and reproducibly inhibit RNase E cleavage (data not shown). This could be due to technical limitations of our assay or it may suggest that other factors are needed to fully reconstruct the process *in vitro*.

S1 overexpression and depletion effects on mRNA are not specific for *cspE*

The data reported above show that ΔL-*cspE* may be degraded by both RNase E-dependent and independent pathways and that S1 overexpression may inhibit RNase E-dependent degradation. To clarify whether RNA protection by S1 was specific for this transcript or could be a more general phenomenon, we analysed *in vivo* other leaderless artificial mRNAs. The *rpsO* gene was used as a backbone of our constructs because it is sensitive to S1 stabilization (6) and its RNase E-dependent degradation pathway has been extensively studied (56). Two constructs were analysed, a leaderless *rpsO* gene (ΔL-*rpsO*::HA) and a λ *cI-rpsO* fusion (carried by plasmid pGM398 and pGM397, respectively; Figure 2A). In both constructs, the region encoding S15 binding site for 16S rRNA (33) was replaced with an in frame HA epitope (Figure 2A). This allowed discriminating transcripts deriving from chromosomal or plasmid alleles with specific probes in northern hybridization.

RNase E was expected to be involved in the decay of the ΔL-*rpsO*::*HA* transcripts, as all known RNase E cleavage

sites mapping in *rpsO* (Figure 2A) are conserved in this construct. To assess if this was indeed the case, we analysed the transcription profile of Δ*L-rpsO*::*HA* construct in the RNase E defective strain. We observed that the transcript covering the region between *rpsOp* and *rpsOt* (Supplementary Figure S5A, P-t, and Supplementary Table S3) and longer RNAs deriving from transcriptional read-through of the *rpsOt* (Supplementary Figure S5A, stars) were clearly stabilized in the *rne*^{ts} strain at 44°C. Thus, Δ*L-rpsO*::*HA* RNA appears to be degraded via an RNase E-dependent pathway. It is very likely that the same holds true also for *cI-rpsO*, as two known RNase E-dependent cleavage sites located respectively immediately upstream and overlapping the *rpsOt* terminator are present in pGM397 construct (Figure 2A).

We then analysed the effect of S1 expression modulation on *rpsO* transcription profile. Leadered *rpsO*$^{+}$ mRNA expressed by the chromosomal allele was stabilized six to seven times by over-expressed S1 in these strains (Supplementary Figure S5B and Table 1). Leaderless transcripts deriving from Δ*L-rpsO*::*HA* and *cI-rpsO* constructs were quite unstable, with half-lives around 1 min, and were strongly stabilized by S1 overexpression (Supplementary Figure S5 and Table 1); in the latter condition, the amount and stability of RNAs expressed by the two constructs that encompass the *rpsOt* intrinsic terminator were also clearly increased (Supplementary Figure S5B, upper panel, stars). Thus, as for Δ*L-cspE* transcripts, overexpression of S1 stabilizes these otherwise very unstable leaderless RNAs by inhibiting their RNase E-dependent decay.

As observed for *cspE*, upon S1 depletion the two leaderless transcripts became 2–3-fold more abundant and slightly more stable, whereas the amount of both the leadered *L-rpsO*::*HA* expressed by pGM396 and *rpsO*$^{+}$ chromosomal transcript decreased to 50–60% and 20%, respectively, of the quantity present before depletion. However, the half-life of the remaining *rpsO*$^{+}$ mRNA did not significantly change irrespective of S1 expression level (Supplementary Figure S5C and Table 1).

Leaderless transcripts co-localize with ribosomes irrespective of translation

The above-mentioned results show that S1 expression modulation, and depletion in particular, differentially affects leadered and leaderless RNA expression and stability. It is possible that differences in ribosome association and/or translation efficiency may contribute to this difference. We thus assayed the association with ribosomes of leadered and leaderless RNAs expressed by the above constructs (Figure 2) in different conditions of S1 expression. To do so, RNA from crude extracts, ribosomal fractions and S100 fractions prepared from different cultures (listed in Figure 5 legend), as described in 'Materials and Methods' section, were analysed by northern blotting (Figure 5). Leadered transcripts were found only in the ribosomal fraction at physiological levels of S1 expression; after S1 overexpression, they were present both in the ribosomal and in the S100 fractions. Leaderless mRNAs were found mainly in the ribosomal fraction before S1 induction and only in the S100 upon S1 overexpression, with the exception of *cI-rpsO* transcript that associated to the ribosomal fraction irrespective of S1 expression levels. This could be explained by the presence in *cI* mRNA of an out of frame AUG (nucleotides 68–70) preceded by a properly positioned SD sequence (57).

Interestingly, S1 depletion did not affect ribosome association of the leaderless transcripts (Figure 5). Moreover, we assayed by western blotting with anti-HA antibodies the translation efficiency of the leadered and leaderless set of constructs tagged with the HA epitope shown in Figure 2. We found that both *L-cspE*::*HA* and *L-rpsO*::*HA* leadered transcripts were translated; the expression of both proteins was sensitive to S1 levels, as it sharply decreased in S1 depletion and, to a lesser extent (about 60% of pre-induction level for *L-rpsO*::*HA* and 50% for *L-cspE*::*HA*), upon S1 overexpression (Figure 6). The leaderless Δ*L-cspE*::*HA* and Δ*L-rpsO*::*HA* transcripts, albeit co-localizing with ribosomes (Figure 5), were detectably translated in none of the different conditions of S1 expression. On the contrary, the amount of CI-RpsO hybrid protein (relative to L4 ribosomal protein amount) did not change in any condition tested, irrespective of S1 levels (Figure 6).

DISCUSSION

S1 protein can act as a negative modulator of translation and RNase E-dependent mRNA decay

In this work, we have investigated S1 role in translation and mRNA stability control by altering S1 expression level. Our data show that S1 overexpression causes polysome disappearance and translation inhibition. Moreover, a sharp increase in the amount of S100 S1 (ribosome-unbound) and cellular re-distribution of mRNA from ribosomal to S100 fractions are observed (see Figures 1C and 5). This suggests that *in vivo* the ribosome-unbound S1 can negatively affect the association between ribosome and mRNA, as already demonstrated *in vitro* for different mRNAs (58). Indeed, if the first step in initiation complex formation requires the interaction between 30S-associated S1 and the mRNA leader region (17,18), S1 binding to high-affinity site(s) in the mRNA leader regions may hamper mRNA binding to S1-containing 30S subunits (22,23) (see Figure 3D). Translation repression by S1 expressed at physiological level has been documented for a couple of *E. coli* genes. In fact, S1 acts as a repressor of its own gene translation by preventing association of its own mRNA to 30S (58,59). *rpsA* mRNA lacks a canonical SD sequence; for this messenger, 30S recruitment could be strictly mediated by 30S-bound S1 and thus efficiently counteracted by free (ribosome-unbound) S1. S1 has been also claimed to repress translation of the dicistronic *rpsB* and *tsf* (encoding elongation factor Ts) mRNA in cooperation with another ribosomal protein, S2 (60). Overexpression appears thus to intensify and extend an otherwise specific activity of S1 as a negative modulator of translation initiation.

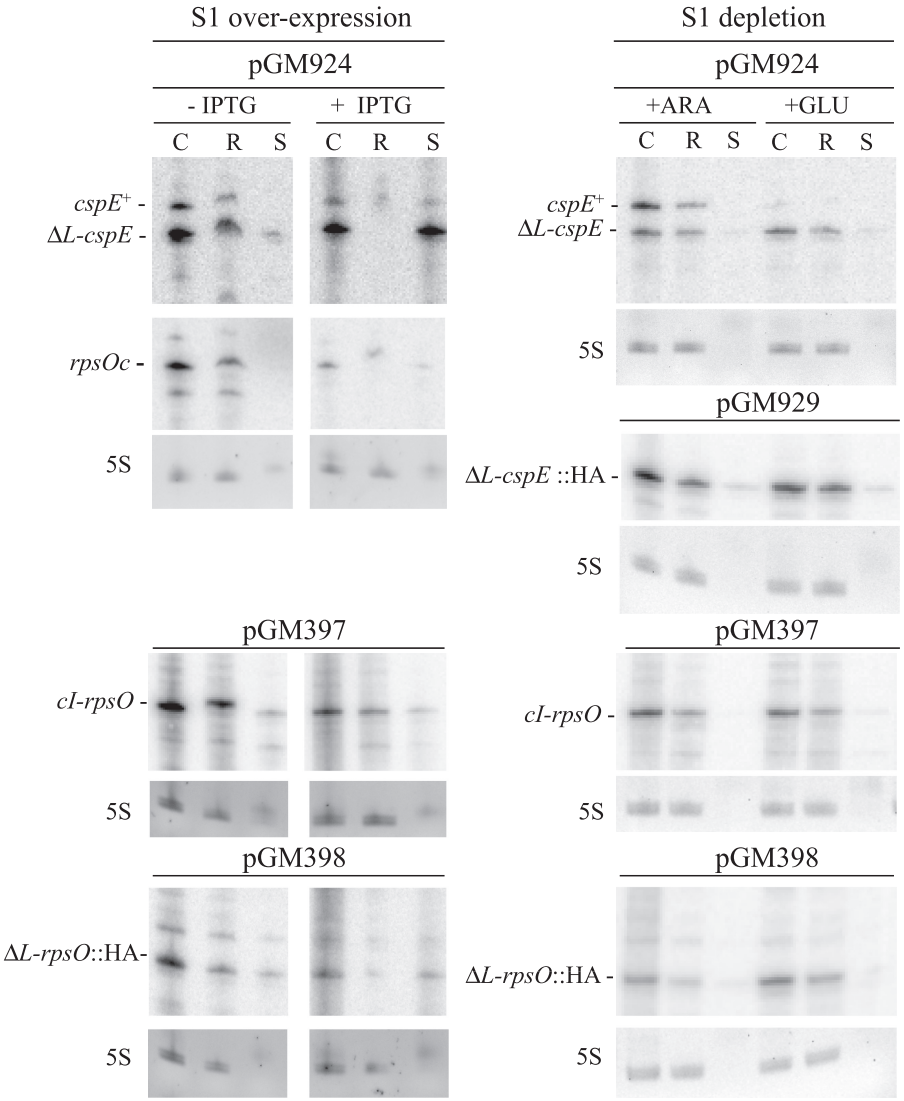

Figure 5. Intracellular distribution of leadered and leaderless mRNAs upon modulation of S1 expression. Northern blotting of RNA samples extracted from crude extracts (C) and from ribosomal (R) and S100 (S) fractions. Cultures of C-1a/pREP4/pQE31-S1 (S1 overexpression) or C-5699 (S1 depletion) strains carrying the additional plasmids listed above the panels were grown as detailed in 'Materials and Methods' section. Identical volumes of the RNA samples were analysed by 6% denaturing polyacrylamide gel electrophoresis, northern blotted and hybridized with the following oligonucleotides. pGM924, oligo 2135 (*cspE* panels) or 2469 (specific for *rpsO* mRNA expressed by the chromosomal gene; *rpsOc* panel); pGM397, pGM398 (S1 depletion) and pGM929, oligo HA; pGM398 (S1 overexpression), oligo 2313 (specific for *rpsO*). Left part, −IPTG, S1 basal; + IPTG, S1 induced. Right part, + ARA, S1 expressed, + GLU, S1 depleted.

Besides preventing the initial association between the mRNA and the ribosome, S1 overexpression may affect translation through a different and still puzzling mechanism. In fact, monosomes accumulation in S1 overexpressing cells suggests that either ribosomal subunits do not dissociate after releasing the mRNA or the 70S–mRNA complex remains associated. The presence of residual leadered mRNA in the ribosomal fractions after S1 induction (see Figure 1C) supports the latter hypothesis. At the moment, we have no experimental hint on a possible mechanism for mRNA trapping on ribosome. One can speculate that S1 dissociates from the ribosome at some point during translation and that overexpression may alter its cycling, preventing mRNA release. Evidences based on S1 stoichiometry determination in polysomes and on its role in translation elongation argue against S1 dissociation during elongation (9,13,61). On the other hand, leaderless mRNAs can be translated *in vitro* by S1-depleted 70S (14). Moreover, to our knowledge, S1 fate during translation termination and ribosome release has never been addressed. The existence of a ribosome-unbound S1 pool, whose magnitude depends on S1 expression level, and the observation that upon S1 overexpression 70S–mRNA–S1 complexes may be stabilized, support S1 recycling at physiological S1 concentration.

In spite of translation inhibition, different transcripts are stabilized by S1 overexpression. This is not due to a general impairment of RNA degradation, since Δ*L-cspE* degradation from the 5′-end by an unknown endonuclease

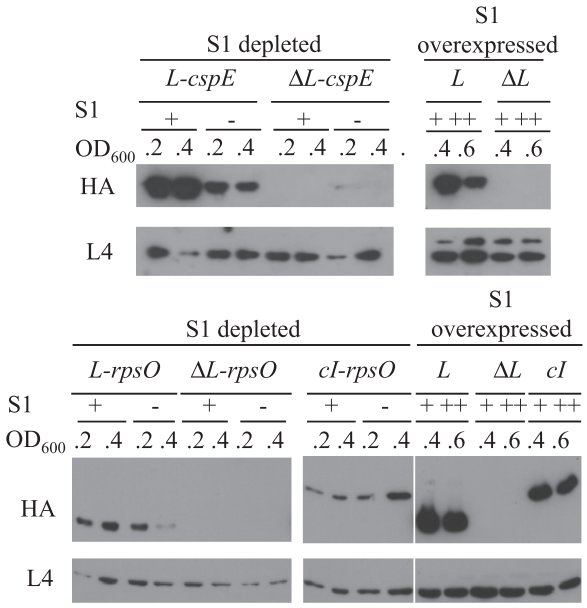

Figure 6. Translation of leadered and leaderless mRNAs upon modulation of S1 expression. Proteins extracted from cultures of C-1a/pREP4/pQE31-S1 (S1 depleted; +, S1 basal; ++, S1 induced) or C-5699 (S1 depleted; +, S1 expressed; −, S1 repressed) strains carrying *cspE*::*HA* (upper panels: *L-cspE*, pGM928; Δ*L-cspE*, pGM929) or *rpsO*::*HA* (lower panels: *L-rpsO*, pGM396; Δ*L-rpsO*, pGM398; *cI-rpsO*, pGM397) plasmids were prepared as detailed in 'Materials and Methods' section. Proteins were separated by 15% denaturing polyacrylamide gel electrophoresis and immunodecorated with antibodies specific for the HA epitope or, as a loading control, for L4 ribosomal protein. For quantitative evaluation of CspE::HA and RpsO::HA expression, both HA- and L4-specific antibodies signals were quantified with ImageQuant (Molecular Dynamics); each HA-specific signal volume was then normalized by the volume of the corresponding L4-specific signal.

is not prevented by S1. Conversely, S1 overexpression inhibits RNase E-dependent decay of our reporter transcripts. Another ribosomal protein, L4, has been involved in mRNA stability control, as it was shown to physically interact with RNase E and negatively regulate its endoribonucleolytic function (62). We cannot rule out that S1 may exert its inhibitory function by physically interacting with RNase E; however, we have not found RNase E among proteins co-purifying with His-tagged S1 (Briani,F., unpublished data). In addition, S1 has been shown to preferentially bind mRNA at A/U- rich single-stranded regions that also constitute potential RNase E cleavage sites (1,22–24). This suggests that S1 may inhibit RNase E decay by directly shielding cleavage site(s).

Our *in vitro* data (see Figure 3D) and data by other groups (22,23,63) suggest that S1 not bound to ribosomes may preferentially interact with sites located in the mRNA leader regions. This interaction may have different consequences on RNA stability depending on the specific decay pathway run by an RNA specie [(64); current models of RNase E degradation modes have been recently reviewed by refs. 44 and 65]. For RNAs degraded predominantly through a wave of cleavages by RNase E moving 5′ to 3′, S1 binding to the 5′-UTR could hinder the first RNase E cut, which is the rate-limiting step in this degradation pathway. This would uncouple translation and decay by protecting the translationally silenced mRNA from degradation. It would be interesting to investigate whether this is indeed the case for *rpsA* and *rpsB-tsf* mRNAs. More in general, in conditions of impaired translation, such as amino acid starvation or cold shock, ribosome-unbound S1 may protect part of cellular transcripts from decay. Best candidates for S1 protection would be transcripts with high-affinity sites for S1 in their leader regions and degraded 5′ to 3′ by RNase E, because they could be sensitive to a relatively modest free S1 increase. Conversely, free S1 binding to the 5′-UTR may result in very fast (possibly co-transcriptional) degradation of mRNAs attacked by RNase E at internal sites, because these sites will be no longer hindered by translating ribosomes. However, S1 binding at ectopic sites (i.e. downstream of the leader region) would allow some molecules to escape degradation, thus stabilizing a share of the mRNA. It has been proposed that RNase E may degrade *rpsO* mRNA predominantly through the 'internal entry' mode (65). Our *in vitro* data suggest that also *cspE* RNA may enter such degradation pathway, since the phosphorylation state of the 5′-end of our probes or even the presence of a leader region seem to marginally affect the *in vitro* degradation efficiency by RNase E. This may explain why, despite the strong half-life increase, the abundance of tested mRNAs does not correspondingly increase or even decreases in S1 over-expressing cells (Table 1) (6).

Ribosomal particles lacking S1 may be present in normally growing cells

Our artificial leaderless Δ*L-cspE* and Δ*L-rpsO*::*HA* RNAs co-fractionate with ribosomes at basal S1 expression, whereas they are present only in S100 fraction in S1 over-expressing cells. Their re-distribution upon S1 overexpression is more drastic than for leadered RNAs, which are, in part, still retained in ribosomal fractions, and may occur through a different mechanism.

Leaderless transcripts enjoy a peculiar translation initiation pathway based on the initial interaction of the terminal AUG with 70S particles (14,20,21). S1 has a documented destabilizing effect on this interaction (14,66). The presence of leaderless mRNAs in the ribosomal fraction at S1 physiological levels suggests that ribosomal particles without S1 may be present in the cells. The slight increase in S1 stoichiometry observed in monosome fractions upon overexpression also favours the idea that S1 could be normally present in slightly sub-stoichiometric amount in 70S particles, as previously suggested (9), and may reach stoichiometry when over-expressed. A conclusive experimental demonstration of this hypothesis would be very challenging, since S1 dissociation from ribosomal particles may occur after cell lysis (10–12). However, the idea that leaderless mRNAs may interact with 70S particles lacking S1 is strengthened by S1 depletion data. In this condition, 70S particles lacking S1 accumulate, probably because of their unusual stability (20,67), and also leaderless mRNAs, which are detectable only in ribosomal fraction, become more abundant, suggesting that in

this condition the share of RNA molecules stabilized by ribosome binding may increase.

In spite of their association with ribosomes, artificial leaderless mRNAs are not detectably translated in any assayed condition, suggesting that these transcripts may establish an unproductive interaction with 70S ribosome. On the contrary, the chimeric *cI-rpsO* mRNA, which contains the 5′-end of the naturally leaderless λ *c*I RNA, is translated both at physiological S1 expression and upon depletion (no conclusion can be drawn about *cI-rpsO* mRNA translation upon overexpression as the 60-min time of S1 induction is likely insufficient to get rid of the protein synthesized before the induction). In agreement with our data, it has been recently reported that a *cI-lacZ* fusion is translated 60-fold more efficiently than a leaderless *lacZ* reporter construct (68). The molecular bases of λ *cI* mRNA properties still remain elusive. However, it has been pointed out that to initiate translation, the terminal AUG of leaderless RNAs should be located at the ribosomal P-site. This would require the RNA to worm its way through the channel between the subunits of the 70S ribosome. The propensity of different transcripts 5′-end to fold into (stable) secondary structures may modulate their ability to enter into the channel and establish a fruitful interaction with the ribosome (14).

SUPPLEMENTARY DATA

Supplementary Data are available at NAR online.

ACKNOWLEDGEMENTS

We thank U. Bläsi and C.O. Gualerzi for providing antibodies, M.V. Sukhodolets for providing plasmids, and the ''National BioResource Project (NIG, Japan): *E. coli*'' for providing bacterial trains. We thank Isabella Moll for critical reading of the manuscript.

FUNDING

Ministero dell'Università e della Ricerca and Università degli Studi di Milano (PRIN 2007); and Università degli Studi di Milano (FIRST2007 and PUR2008). Funding for open access charge: Università degli Studi di Milano.

Conflict of interest statement. None declared.

REFERENCES

1. Kaberdin,V.R. and Bläsi,U. (2006) Translation initiation and the fate of bacterial mRNAs. *FEMS Microbiol. Rev.*, **30**, 967–979.
2. Deana,A. and Belasco,J.G. (2005) Lost in translation: the influence of ribosomes on bacterial mRNA decay. *Genes Dev.*, **19**, 2526–2533.
3. Draper,D.E., Pratt,C.W. and von Hippel,P.H. (1977) *Escherichia coli* ribosomal protein S1 has two polynucleotide binding sites. *Proc. Natl Acad. Sci. USA*, **74**, 4786–4790.
4. Kalapos,M.P., Paulus,H. and Sarkar,N. (1997) Identification of ribosomal protein S1 as a poly(A) binding protein in *Escherichia coli*. *Biochimie*, **79**, 493–502.
5. Feng,Y., Huang,H., Liao,J. and Cohen,S.N. (2001) *Escherichia coli* poly(A)-binding proteins that interact with components of degradosomes or impede RNA decay mediated by polynucleotide phosphorylase and RNase E. *J. Biol. Chem.*, **276**, 31651–31656.
6. Briani,F., Curti,S., Rossi,F., Carzaniga,T., Mauri,P. and Dehò,G. (2008) Polynucleotide phosphorylase hinders mRNA degradation upon ribosomal protein S1 overexpression in *Escherichia coli*. *RNA.*, **14**, 2417–2429.
7. Held,W.A., Mizushima,S. and Nomura,M. (1973) Reconstitution of *Escherichia coli* 30S ribosomal subunits from purified molecular components. *J. Biol. Chem.*, **248**, 5720–5730.
8. Subramanian,A.R. (1983) Structure and functions of ribosomal protein S1. *Prog. Nucleic Acid Res. Mol. Biol.*, **28**, 101–142.
9. van Knippenberg,P.H., Hooykaas,P.J. and van Duin,J. (1974) The stoichiometry of *E. coli* 30S ribosomal protein S1 on *in vivo* and *in vitro* polyribosomes. *FEBS Lett.*, **41**, 323–326.
10. Szer,W., Hermoso,J.M. and Leffler,S. (1975) Ribosomal protein S1 and polypeptide chain initiation in bacteria. *Proc. Natl Acad. Sci. USA*, **72**, 2325–2329.
11. Robertson,W.R., Dowsett,S.J. and Hardy,S.J. (1977) Exchange of ribosomal proteins among the ribosomes of *Escherichia coli*. *Mol. Gen. Genet.*, **157**, 205–214.
12. Subramanian,A.R. and van Duin,J. (1977) Exchange of individual ribosomal proteins between ribosomes as studied by heavy isotope-transfer experiments. *Mol. Gen. Genet.*, **158**, 1–9.
13. Sørensen,M.A., Fricke,J. and Pedersen,S. (1998) Ribosomal protein S1 is required for translation of most, if not all, natural mRNAs in *Escherichia coli in vivo*. *J. Mol. Biol.*, **280**, 561–569.
14. Moll,I., Grill,S., Gualerzi,C.O. and Bläsi,U. (2002) Leaderless mRNAs in bacteria: surprises in ribosomal recruitment and translational control. *Mol. Microbiol.*, **43**, 239–246.
15. Kaberdina,A.C., Szaflarski,W., Nierhaus,K.H. and Moll,I. (2009) An unexpected type of ribosomes induced by kasugamycin: a look into ancestral times of protein synthesis? *Mol. Cell*, **33**, 227–236.
16. Tedin,K., Resch,A. and Bläsi,U. (1997) Requirements for ribosomal protein S1 for translation initiation of mRNAs with and without a 5′ leader sequence. *Mol. Microbiol.*, **25**, 189–199.
17. Hauryliuk,V. and Ehrenberg,M. (2006) Two-step selection of mRNAs in initiation of protein synthesis. *Mol. Cell*, **22**, 155–156.
18. Studer,S.M. and Joseph,S. (2006) Unfolding of mRNA secondary structure by the bacterial translation initiation complex. *Mol. Cell*, **22**, 105–115.
19. Farwell,M.A., Roberts,M.W. and Rabinowitz,J.C. (1992) The effect of ribosomal protein S1 from *Escherichia coli* and *Micrococcus luteus* on protein synthesis *in vitro* by *E. coli* and *Bacillus subtilis*. *Mol. Microbiol.*, **6**, 3375–3383.
20. Moll,I., Hirokawa,G., Kiel,M.C., Kaji,A. and Bläsi,U. (2004) Translation initiation with 70S ribosomes: an alternative pathway for leaderless mRNAs. *Nucleic Acids Res.*, **32**, 3354–3363.
21. Udagawa,T., Shimizu,Y. and Ueda,T. (2004) Evidence for the translation initiation of leaderless mRNAs by the intact 70S ribosome without its dissociation into subunits in eubacteria. *J. Biol. Chem.*, **279**, 8539–8546.
22. Sengupta,J., Agrawal,R.K. and Frank,J. (2001) Visualization of protein S1 within the 30S ribosomal subunit and its interaction with messenger RNA. *Proc. Natl Acad. Sci. USA*, **98**, 11991–11996.
23. Boni,I.V., Isaeva,D.M., Musychenko,M.L. and Tzareva,N.V. (1991) Ribosome-messenger recognition: mRNA target sites for ribosomal protein S1. *Nucleic Acids Res.*, **19**, 155–162.
24. Komarova,A.V., Tchufistova,L.S., Dreyfus,M. and Boni,I.V. (2005) AU-rich sequences within 5′ untranslated leaders enhance translation and stabilize mRNA in *Escherichia coli*. *J. Bacteriol.*, **187**, 1344–1349.
25. Sasaki,I. and Bertani,G. (1965) Growth abnormalities in Hfr derivatives of *Escherichia coli* strain C. *J. Gen. Microbiol.*, **40**, 365–376.
26. Carzaniga,T., Briani,F., Zangrossi,S., Merlino,G., Marchi,P. and Dehò,G. (2009) Autogenous regulation of *Escherichia coli* polynucleotide phosphorylase expression revisited. *J. Bacteriol.*, **191**, 1738–1748.
27. Datsenko,K.A. and Wanner,B.L. (2000) One-step inactivation of chromosomal genes in *Escherichia coli* K-12 using PCR products. *Proc. Natl Acad. Sci. USA*, **97**, 6640–6645.

28. Baba,T., Ara,T., Hasegawa,M., Takai,Y., Okumura,Y., Baba,M., Datsenko,K.A., Tomita,M., Wanner,B.L. and Mori,H. (2006) Construction of *Escherichia coli* K-12 in-frame, single-gene knockout mutants: the Keio collection. *Mol. Syst. Biol.*, **2**, 2006.
29. Sukhodolets,M.V. and Garges,S. (2003) Interaction of *Escherichia coli* RNA polymerase with the ribosomal protein S1 and the Sm-like ATPase Hfq. *Biochemistry*, **42**, 8022–8034.
30. Zangrossi,S., Briani,F., Ghisotti,D., Regonesi,M.E., Tortora,P. and Dehò,G. (2000) Transcriptional and post-transcriptional control of polynucleotide phosphorylase during cold acclimation in *Escherichia coli*. *Mol. Microbiol.*, **36**, 1470–1480.
31. Lessl,M., Balzer,D., Lurz,R., Waters,V.L., Guiney,D.G. and Lanka,E. (1992) Dissection of IncP conjugative plasmid transfer: definition of the transfer region Tra2 by mobilization of the Tra1 region in trans. *J. Bacteriol.*, **174**, 2493–2500.
32. Briani,F., Zangrossi,S., Ghisotti,D. and Dehò,G. (1996) A Rho-dependent transcription termination site regulated by bacteriophage P4 RNA immunity factor. *Virology*, **223**, 57–67.
33. Ehresmann,C., Ehresmann,B., Ennifar,E., Dumas,P., Garber,M., Mathy,N., Nikulin,A., Portier,C., Patel,D. and Serganov,A. (2004) Molecular mimicry in translational regulation: the case of ribosomal protein S15. *RNA Biol.*, **1**, 66–73.
34. Blattner,F.R., Plunkett,G. III, Bloch,C.A., Perna,N.T., Burland,V., Riley,M., Collado-Vides,J., Glasner,J.D., Rode,C.K., Mayhew,G.F. *et al.* (1997) The complete genome sequence of *Escherichia coli* K-12. *Science*, **277**, 1453–1462.
35. Ghisotti,D., Chiaramonte,R., Forti,F., Zangrossi,S., Sironi,G. and Dehò,G. (1992) Genetic analysis of the immunity region of phage-plasmid P4. *Mol. Microbiol.*, **6**, 3405–3413.
36. Dehò,G., Zangrossi,S., Sabbattini,P., Sironi,G. and Ghisotti,D. (1992) Bacteriophage P4 immunity controlled by small RNAs *via* transcription termination. *Mol. Microbiol.*, **6**, 3415–3425.
37. Briani,F., Del Favero,M., Capizzuto,R., Consonni,C., Zangrossi,S., Greco,C., De Gioia,L., Tortora,P. and Dehò,G. (2007) Genetic analysis of polynucleotide phosphorylase structure and functions. *Biochimie*, **89**, 145–157.
38. Forti,F., Sabbattini,P., Sironi,G., Zangrossi,S., Dehò,G. and Ghisotti,D. (1995) Immunity determinant of phage-plasmid P4 is a short processed RNA. *J. Mol. Biol.*, **249**, 869–878.
39. Charollais,J., Pflieger,D., Vinh,J., Dreyfus,M. and Iost,I. (2003) The DEAD-box RNA helicase SrmB is involved in the assembly of 50S ribosomal subunits in *Escherichia coli*. *Mol. Microbiol.*, **48**, 1253–1265.
40. Mauri,P. and Dehò,G. (2008) A proteomic approach to the analysis of RNA degradosome composition in *Escherichia coli*. *Methods Enzymol.*, **447**, 99–117.
41. Lopez,P.J., Marchand,I., Joyce,S.A. and Dreyfus,M. (1999) The C-terminal half of RNase E, which organizes the *Escherichia coli* degradosome, participates in mRNA degradation but not rRNA processing *in vivo*. *Mol. Microbiol.*, **33**, 188–199.
42. Leroy,A., Vanzo,N.F., Sousa,S., Dreyfus,M. and Carpousis,A.J. (2002) Function in *Escherichia coli* of the non-catalytic part of RNase E: role in the degradation of ribosome-free mRNA. *Mol. Microbiol.*, **45**, 1231–1243.
43. Blundell,M.R. and Wild,D.G. (1971) Altered ribosomes after inhibition of *Escherichia coli* by rifampicin. *Biochem. J.*, **121**, 391–398.
44. Carpousis,A.J., Luisi,B.F. and McDowall,K.J. (2009) Endonucleolytic initiation of mRNA decay in *Escherichia coli*. *Prog. Mol. Biol. Transl. Sci.*, **85**, 91–135.
45. Uppal,S., Akkipeddi,V.S. and Jawali,N. (2008) Post-transcriptional regulation of *cspE* in *Escherichia coli*: involvement of the short 5′-untranslated region. *FEMS Microbiol. Lett.*, **279**, 83–91.
46. Perwez,T. and Kushner,S.R. (2006) RNase Z in *Escherichia coli* plays a significant role in mRNA decay. *Mol. Microbiol.*, **60**, 723–737.
47. Rapaport,L.R. and Mackie,G.A. (1994) Influence of translational efficiency on the stability of the mRNA for ribosomal protein S20 in *Escherichia coli*. *J. Bacteriol.*, **176**, 992–998.
48. Tock,M.R., Walsh,A.P., Carroll,G. and McDowall,K.J. (2000) The CafA protein required for the 5′-maturation of 16 S rRNA is a 5′-end-dependent ribonuclease that has context-dependent broad sequence specificity. *J. Biol. Chem.*, **275**, 8726–8732.
49. Condon,C. (2006) Shutdown decay of mRNA. *Mol. Microbiol.*, **61**, 573–583.
50. Ruckman,J., Ringquist,S., Brody,E. and Gold,L. (1994) The bacteriophage T4 regB ribonuclease. Stimulation of the purified enzyme by ribosomal protein S1. *J. Biol. Chem.*, **269**, 26655–26662.
51. Uzan,M. and Miller,E.S. (2010) Post-transcriptional control by bacteriophage T4: mRNA decay and inhibition of translation initiation. *Virol. J.*, **7**, 360.
52. Odaert,B., Saida,F., Aliprandi,P., Durand,S., Crechet,J.B., Guerois,R., Laalami,S., Uzan,M. and Bontems,F. (2007) Structural and functional studies of RegB, a new member of a family of sequence-specific ribonucleases involved in mRNA inactivation on the ribosome. *J. Biol. Chem.*, **282**, 2019–2028.
53. Mackie,G.A. (1998) Ribonuclease E is a 5′-end-dependent endonuclease. *Nature*, **395**, 720–723.
54. Jiang,X., Diwa,A. and Belasco,J.G. (2000) Regions of RNase E important for 5′-end-dependent RNA cleavage and autoregulated synthesis. *J. Bacteriol.*, **182**, 2468–2475.
55. Hankins,J.S., Zappavigna,C., Prud'homme-Genereux,A. and Mackie,G.A. (2007) Role of RNA structure and susceptibility to RNase E in regulation of a cold shock mRNA, *cspA* mRNA. *J. Bacteriol.*, **189**, 4353–4358.
56. Arraiano,C.M., Andrade,J.M., Domingues,S., Guinote,I.B., Malecki,M., Matos,R.G., Moreira,R.N., Pobre,V., Reis,F.P., Saramago,M. *et al.* (2010) The critical role of RNA processing and degradation in the control of gene expression. *FEMS Microbiol. Rev.*, **34**, 883–923.
57. Tedin,K., Moll,I., Grill,S., Resch,A., Graschopf,A., Gualerzi,C.O. and Bläsi,U. (1999) Translation initiation factor 3 antagonizes authentic start codon selection on leaderless mRNAs. *Mol. Microbiol.*, **31**, 67–77.
58. Boni,I.V., Artamonova,V.S., Tzareva,N.V. and Dreyfus,M. (2001) Non-canonical mechanism for translational control in bacteria: synthesis of ribosomal protein S1. *EMBO J.*, **20**, 4222–4232.
59. Skorski,P., Leroy,P., Fayet,O., Dreyfus,M. and Hermann-Le Denmat,S. (2006) The highly efficient translation initiation region from the *Escherichia coli rpsA* gene lacks a Shine–Dalgarno element. *J. Bacteriol.*, **188**, 6277–6285.
60. Aseev,L.V., Levandovskaya,A.A., Tchufistova,L.S., Scaptsova,N.V. and Boni,I.V. (2008) A new regulatory circuit in ribosomal protein operons: S2-mediated control of the *rpsB-tsf* expression *in vivo*. *RNA*, **14**, 1882–1894.
61. Potapov,A.P. and Subramanian,A.R. (1992) Effect of *E. coli* ribosomal protein S1 on the fidelity of the translational elongation step: reading and misreading of poly(U) and poly(dT). *Biochem. Int.*, **27**, 745–753.
62. Singh,D., Chang,S.J., Lin,P.H., Averina,O.V., Kaberdin,V.R. and Lin-Chao,S. (2009) Regulation of ribonuclease E activity by the L4 ribosomal protein of *Escherichia coli*. *Proc. Natl Acad. Sci. USA*, **106**, 864–869.
63. Ringquist,S., Jones,T., Snyder,E.E., Gibson,T., Boni,I. and Gold,L. (1995) High-affinity RNA ligands to *Escherichia coli* ribosomes and ribosomal protein S1: comparison of natural and unnatural binding sites. *Biochemistry*, **34**, 3640–3648.
64. Baker,K.E. and Mackie,G.A. (2003) Ectopic RNase E sites promote bypass of 5′-end-dependent mRNA decay in *Escherichia coli*. *Mol. Microbiol.*, **47**, 75–88.
65. Dreyfus,M. (2009) Killer and protective ribosomes. *Prog. Mol. Biol. Transl. Sci.*, **85**, 423–466.
66. Moll,I., Resch,A. and Bläsi,U. (1998) Discrimination of 5′-terminal start codons by translation initiation factor 3 is mediated by ribosomal protein S1. *FEBS Lett.*, **436**, 213–217.
67. Grill,S., Moll,I., Hasenohrl,D., Gualerzi,C.O. and Bläsi,U. (2001) Modulation of ribosomal recruitment to 5′-terminal start codons by translation initiation factors IF2 and IF3. *FEBS Lett.*, **495**, 167–171.
68. Krishnan,K.M., Van,E.W. III and Janssen,G.R. (2010) Proximity of the start codon to a leaderless mRNA's 5′ terminus is a strong positive determinant of ribosome binding and expression in *Escherichia coli*. *J. Bacteriol.*, **192**, 6482–6485.
69. Régnier,P. and Portier,C. (1986) Initiation, attenuation and RNase III processing of transcripts from the *Escherichia coli* operon encoding ribosomal protein

S15 and polynucleotide phosphorylase. *J. Mol. Biol.*, **187**, 23–32.
70. Walz,A., Pirrotta,V. and Ineichen,K. (1976) Lambda repressor regulates the switch between P_R and P_{RM} promoters. *Nature*, **262**, 665–669.
71. Régnier,P. and Hajnsdorf,E. (1991) Decay of mRNA encoding ribosomal protein S15 of *Escherichia coli* is initiated by an RNase E-dependent endonucleolytic cleavage that removes the 3′ stabilizing stem and loop structure. *J. Mol. Biol.*, **217**, 283–292.
72. Hajnsdorf,E. and Régnier,P. (1999) *E. coli* RpsO mRNA decay: RNase E processing at the beginning of the coding sequence stimulates poly(A)-dependent degradation of the mRNA. *J. Mol. Biol.*, **286**, 1033–1043.